

Crystallization mechanism and microstructure evolution of $\text{Li}_2\text{O}-\text{Al}_2\text{O}_3-\text{SiO}_2$ glass-ceramics with Ta_2O_5 as nucleating agent

Yaohui Li · Kaiming Liang · Bo Xu ·
JianWei Cao

Received: 28 September 2009 / Accepted: 3 November 2009 / Published online: 2 December 2009
© Akadémiai Kiadó, Budapest, Hungary 2009

Abstract $\text{Li}_2\text{O}-\text{Al}_2\text{O}_3-\text{SiO}_2$ glass-ceramics were prepared with Ta_2O_5 as nucleating agent, the crystallization mechanism and microstructure evolution were investigated by DTA, XRD, and SEM technologies. With increasing amount of Ta_2O_5 from 2 to 6 mol%, the crystallization activation energy decreased from 297.73 to 218.66 kJ mol⁻¹, while the crystallization index increased from 1.76 to 3.39. In addition, the cluster of dendritic crystals and lamellar structure obtained in T-2 glass-ceramics indicated a typical two-dimensional crystallization mechanism, and the formation of spherical β -quartz solid solution in T-4 specimens, with average size of 50–70 nm, was mainly due to bulk crystallization mechanism. It was considered that Ta_2O_5 promoted the nucleation and crystallization of LAS glass by precipitating the crystalline precursor phase of Ta_2O_5 , which acted as nuclei for the subsequent crystal growth. Eventually, the diffusion and crystallization process, microstructure morphology, as well as the secondary grain growth were also investigated.

Keywords Glass ceramics · Crystallization · Microstructure-final · Grain growth · Ta_2O_5

Introduction

Glass-ceramics are polycrystalline materials formed by a well-controlled crystallization heat treatment of appropriate parent glass, and properties of glass-ceramics, related to the crystalline phase and microstructure, mainly depend on the addition of nucleating agents [1]. The controlled glass crystallization can be traced back to the original work of Stookey [2], who showed that efficient internal nucleation of the glass enabled a development of the homogeneous, fine-grained microstructure.

Recently, the $\text{Li}_2\text{O}-\text{Al}_2\text{O}_3-\text{SiO}_2$ (LAS) glass-ceramics have come into scientific and economic focus due to its very low thermal expansion coefficient and high visible transparency [3, 4], and many studies on the crystallization and microstructure evolution have been performed [5–9]. Many of the superior properties of internally nucleated LAS glass-ceramics attributed to the fine-grained microstructure can be obtained through optimizing the heat treatment of glass with added nucleating agents [10–13] (such as TiO_2 , ZrO_2 , or their mixture). For specimens containing more than 2 wt% TiO_2 , phase separation occurred on cooling from the melt, and subsequent reheating caused the formation of a large number of titania-rich crystals approximately 5 nm in diameter, which acted as sites of heterogeneous nucleation for volume crystallization of β -quartz solid solution (s.s.). Instead of phase separation, a different mechanism of nucleation was assigned as the precipitation of the precursor nuclei of small crystallites, e.g., ZrTiO_4 , as the precursor nuclei for crystallization [14, 15]. Though the details of nucleating agents effected the process of nucleation and crystallization are still controversial, $\text{TiO}_2 + \text{ZrO}_2$ are the most important commonly used nucleating agents in promoting the crystallization of $\text{Li}_2\text{O}-\text{Al}_2\text{O}_3-\text{SiO}_2$ glass, and give a general outlook of crystallization: phase separation,

Y. Li (✉) · K. Liang · B. Xu · J. Cao
Department of material Science and Engineering, Tsinghua University, 100084 Beijing, China
e-mail: liyahui05@mails.thu.edu.cn

K. Liang
e-mail: lkm-dms@mails.thu.edu.cn

B. Xu
e-mail: xubo06@mails.thu.edu.cn

J. Cao
e-mail: caojw05@mails.thu.edu.cn

followed by formation of precursor nuclei, and then nucleation and growth of β -quartz s.s phase on the sites of $ZrTiO_4$ crystallites.

Moreover, several other agents (P_2O_5 and F^-) were also investigated due to their effect on crystallization [16, 17]. Specially, Ta_2O_5 has been introduced as an effective nucleating agent by Hsu and Speyer [18], who demonstrated the role of Ta_2O_5 in the devitrification process of LAS glass by comparing with TiO_2 , the crystalline precursor phases (e.g., $LiTa_3O_8$ and Ta_2O_5) were found and considered as the reason for crystallization. The influence of Ta_2O_5 additions on the thermal properties and crystallization kinetics was also studied in other glass system [19]. However, there are few reports about the effects of Ta_2O_5 in glasses, and no work has clearly demonstrated the crystallization mechanism, phase equilibrium, microstructure morphology, and the properties of the LAS glass-ceramics with Ta_2O_5 as nucleating agent.

In this study, we followed a novel investigation of crystallization mechanism and microstructure in LAS glass system with different amount of Ta_2O_5 . The crystallization kinetics, phase transition, microstructure evolution, and even the grain growth were discussed using the differential thermal analysis (DTA), X-ray diffraction (XRD), and scanning electron microscopy (SEM) techniques. This research is a part of the preliminary work aimed at the possibilities of obtaining large amounts of β -quartz s.s with fine-grained structure and similar properties using Ta_2O_5 , instead of TiO_2 and ZrO_2 as nucleating agents.

Experiments

The LAS glass compositions are very close to the stoichiometric proportion eucryptite $Li_2O-Al_2O_3-SiO_2$, and varying amounts of Ta_2O_5 (2, 4, and 6 mol%) are introduced as the nucleation agents (Table 1). Analytical reagents of Li_2CO_3 , SiO_2 , and Al_2O_3 were selected as raw materials. The mixtures were homogenized by dry ball-milling and then melted at 1,600 °C for 4 h. The melts were subsequently poured onto steel plates to obtain homogeneous glass samples. Glass patties were cut and

Table 1 Chemical composition of glasses with different amounts of nucleating agent

Sample no.	$Ta_2O_5/\text{mol}\%$	Chemical composition/mass%			
		Li_2O	Al_2O_3	SiO_2	Ta_2O_5
T-0	–	8.02	27.39	64.59	–
T-2	2.00	6.99	23.96	56.35	12.70
T-4	4.00	6.19	21.15	49.77	22.89
T-6	6.00	5.50	18.84	44.29	31.28

then subjected to heat treatments (800, 850, 900, and 1,000 °C/1 h) at the heating rate of 5 °C/min to prepare the glass-ceramics specimens.

In order to determine the crystallization temperature and assess the nonisothermal crystallization kinetics, the three type samples were subjected to a differential thermal analyzer (STA, 409C, Netzsch, Germany) with alumina as the reference at different heating rates (5, 10, 15, and 20 °C/min) between ambient temperatures to 1,100 °C. In order to reduce any effects from surface-controlled crystallization, glass shivers (equal mass about 60 mg) with a particle size ~400 μm , instead of superfine glass powder, were used for all measurements.

The XRD patterns were recorded for crystalline phases utilizing a X-ray diffractometer (D/Max 2500, Rigaku, Germany) operating at 40 kV and 200 mA, using $CuK\alpha$ radiation. In addition, the average sizes of the crystallites were also calculated using the Scherrer formula, applied to the analytical diffraction peak profiles, as already have been used in microstructural studies of LAS glass-ceramics [4]. The intensity of diffraction for the finely powdered crystallized samples was collected with a step size of 0.02° in the preset-time mode (2 s), and the reversed convolution method was employed to correct the measured peak profiles broadening with instrumental effects.

The microstructure and morphology of the glass-ceramics were observed by a scanning electron microscope (JSM-6400, Oxford) at an accelerating voltage of 25 kV. The samples were mechanically ground and polished, and then etched (2% HF for 1 min) to reveal the grain boundaries. The samples were gold-coated and observed with a cold stage by liquid nitrogen to avoid undesirable thermal effects.

Results and discussion

DTA results

As shown in Fig. 1, a series of glass samples with different amount of Ta_2O_5 is carried out for DTA testing at various heating rates in the range of 5–20 °C/min. As expected, no obvious exothermic reaction appears in glasses with Ta_2O_5 content less than 2 mol% (T-0), whereas an unambiguous exothermal peak is observed for each pattern of T-2, T-4, and T-6 specimens in temperature range 850–1,000 °C. These peaks correspond to the crystallization of a β -quartz s.s phase (identified by XRD and discussed subsequently). Obviously, the exothermic peaks shift to lower temperature with the increase of Ta_2O_5 content from approximately 960 °C for T-2 glass to 900 °C of T-4 sample, and even to 877 °C of glass with 6 mol% Ta_2O_5 at the heating rate of 10 °C/min. Furthermore, the peak profiles also show a

Fig. 1 DTA curves of the LAS glasses containing different amounts of Ta_2O_5 . **a** T-0, **b** T-2, **c** T-4, and **d** T-6

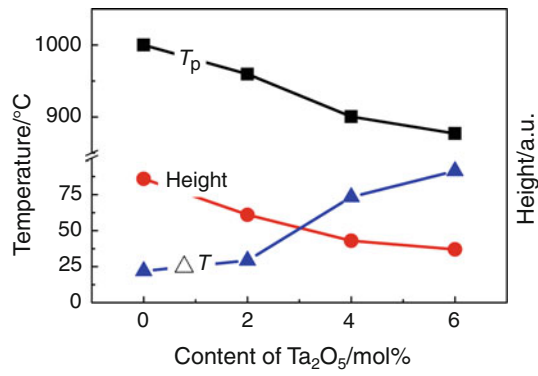
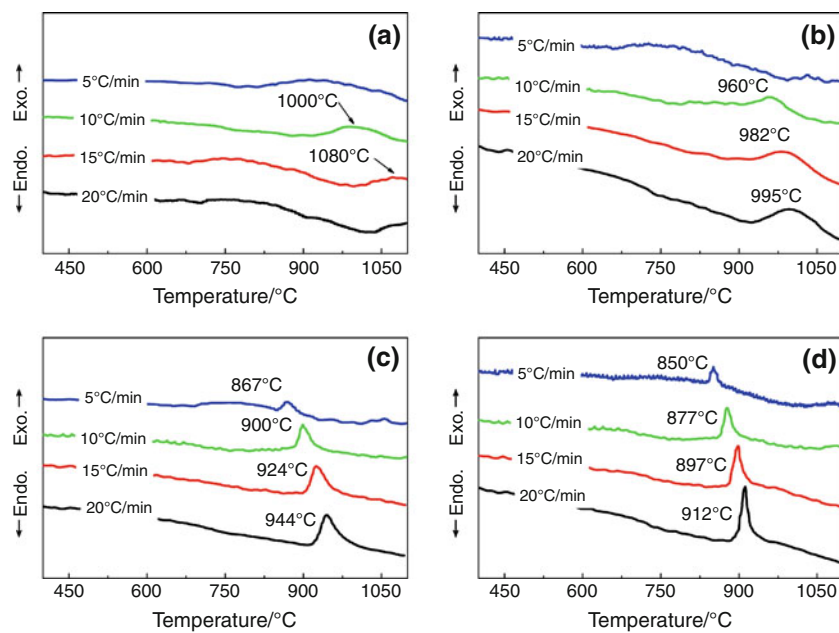


Fig. 2 Plots of DTA peak temperature (T_p), peak height, and half-height width (ΔT) versus Ta_2O_5 (heating rate: 10 °C/min)

strong dependence on the amount of Ta_2O_5 and the heating rate. For instance, the alterations of exothermal peak features for the heating rate of 10 °C/min are shown in Fig. 2. The decrease of T_p and the increase of peak height, both related to the thermal stability, mean that the crystallization of β -quartz s.s becomes much easier and appears at lower temperature with the increase of Ta_2O_5 content. The width of exothermic peak, associated with the reaction rate, indicates that Ta_2O_5 addition accelerates the process of crystallization. Hence, the addition of Ta_2O_5 promotes the crystallization of β -quartz s.s efficiently, and the different features of the DTA curves of T-2, T-4, and T-6 samples are probably caused by different mechanism of nucleation and crystallization in the tantalum-rich glasses.

Nonisothermal kinetics of crystallization

DTA results can explain comprehensive information about the crystallization behavior [20–22], and the isothermal experimental data can be interpreted by the well-established Johnson–Mehl–Avrami equation to assess the crystallization kinetics [23–25]. In general, the crystallization active energy (E) can be obtained by using the Kissinger [26] expression as follows:

$$\ln\left(\frac{T_p^2}{\alpha}\right) = \frac{E}{RT_p} + \ln\frac{E}{R} - \ln v \quad (1)$$

where T_p is the crystallization peak maximum temperature, α is the DTA heating rate (°C/min), R is the gas constant, and v is the frequency factor.

With the values of activation energy, the Avrami parameter (n), related to the mechanism of crystallization, can be derived from the Augis–Bennett equation [27]:

$$n = \frac{2.5}{\Delta T} \times \frac{RT_p^2}{E} \quad (2)$$

where ΔT is the half-height width of the crystallization exothermic peak.

Figure 3 shows the plots of $\ln(T_p^2/\alpha)$ versus $1/T_p$, expected to linear, and the values of E and v derived from the slope and intercept are listed in Table 2. With the increase of Ta_2O_5 content, values of E and the frequency factor v change from 297.73 kJ mol⁻¹, 3.4×10^{11} min⁻¹ to 218.66 kJ mol⁻¹, 1.7×10^9 min⁻¹, respectively. Both

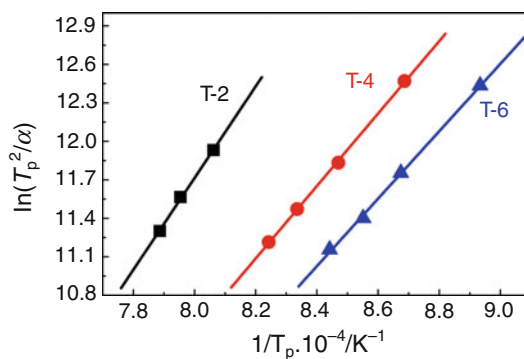


Fig. 3 Plots of $\ln(T_p^2/\alpha)$ versus $1/T_p$ for LAS glasses with different amounts of Ta_2O_5

the lower activation energy and the frequency factor are of great benefit to the crystallization of LAS glass. The values of n , depending upon the actual crystallization mechanism, for three series of glasses are 1.76, 2.84, and 3.39, respectively. These values indicate that the crystallization mechanism changes from surface crystallization to internal crystallization with increasing amount of Ta_2O_5 .

Phase identification and transition

According to the DTA analysis, the crystallization process can also be traced from the crystalline phase identification and transition detected by XRD measurement. Figure 4 shows the powder XRD patterns of T-2, T-4, and T-6 samples under an isothermal heat treatment at different temperatures. It is obvious that Ta_2O_5 influences the behavior of crystallization and phase transformation drastically. Heating experience shows that the LAS glass without nucleating agent heated at 1,000 °C still appears transparent, which indicates that the parent glass has good thermal stability. For T-2 specimens (Fig. 4a), no sharp diffraction peak corresponding to any crystalline phase is detected below 900 °C, and then β -quartz s.s is identified after heat treatment at 1,000 °C for 1 h, along with the β -spodumene s.s and AlTaO_4 crystalline phase having lower diffraction intensity. However, the addition of 4 mol% Ta_2O_5 in LAS glass gives large amount of β -quartz s.s after heat-treated at 850 °C/1 h, while a coexisting minor phase Ta_2O_5 is also observed in Fig. 4b. With increasing temperature, the amount of β -spodumene s.s and AlTaO_4

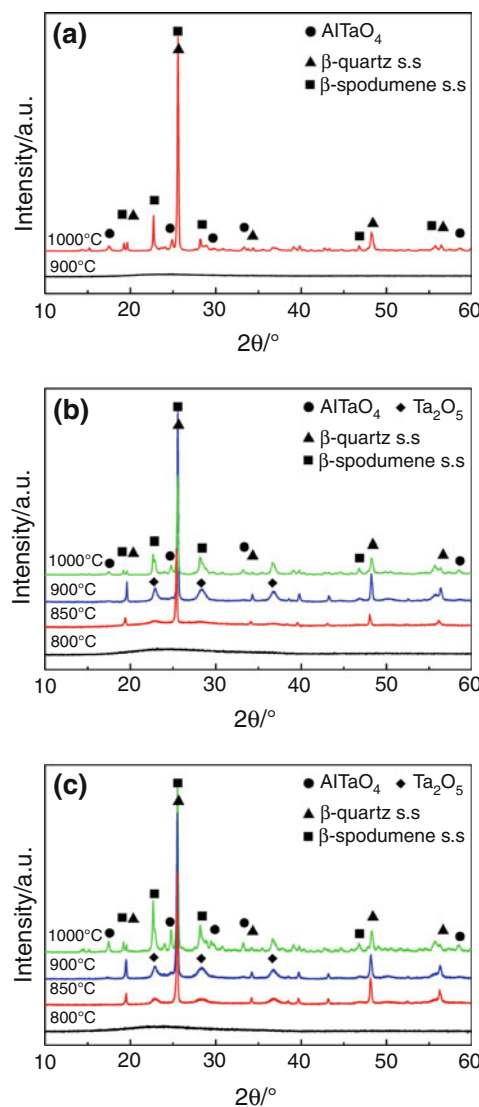


Fig. 4 XRD patterns of the series of glasses crystallized at different temperatures for 1 h. **a** T-2, **b** T-4, and **c** T-6

crystallites increase slightly with the expense of β -quartz s.s and Ta_2O_5 , respectively. As a result, heat treatment at 1,000 °C for 1 h produces a polyphase glass-ceramics composed of four crystalline phases. With the addition of more Ta_2O_5 (6 mol%), as shown in Fig. 4c, crystalline phase appears at a much lower temperature, and the behavior of phase transition is similar to that of T-4

Table 2 Values of T_p , E , v , and n for three different glasses

Sample No.	$T_p/^\circ\text{C}$				$E/\text{kJ mol}^{-1}$	v/min^{-1}	n
	5 °C/min	10 °C/min	15 °C/min	20 °C/min			
T-2	–	958.7	980.6	996.9	297.73 ± 12.05	3.4×10^{11}	1.76 ± 0.07
T-4	867.5	899.1	924.2	944.8	234.83 ± 3.59	5.0×10^9	2.84 ± 0.04
T-6	850.3	877.3	897.2	911.8	218.66 ± 5.07	1.7×10^9	3.39 ± 0.08

samples. Figure 5 shows the XRD patterns of T-4 sample at different temperature under a nonisothermal heat treatment from 800 to 1,050 °C at the heating rate of 5 °C/min. The β -quartz s.s, Ta_2O_5 , β -spodumene s.s, and $AlTaO_4$ are also identified distinctly, and the diffraction intensity, relating to the crystallinity, increases gradually with increasing temperature. The broad diffraction peaks with lower intensity, corresponding to Ta_2O_5 , can be interpreted by a different mechanism of crystallization and growth of Ta_2O_5 crystalline phase in tantalum-rich glasses.

According to the XRD results, the precipitation of crystalline phases is strongly temperature dependent, and the Ta_2O_5 has a pronounced influence on crystallization behaviors. These results are in agreement with the DTA analysis. Thus, Ta_2O_5 addition, 4 mol%, is suitable for promoting crystallization of LAS glass, and a range 850–900 °C seems to be an appropriate temperature for preparation of glass-ceramics with major crystalline phase of β -quartz s.s.

Crystallization mechanism

As shown in Fig. 5, the Ta_2O_5 phase, corresponding to the broad peaks at about 22.8°, 28.3°, and 36.7°, is observed as a minor crystalline phase to form along with the major phase of β -quartz s.s in a large range of temperature. The same crystalline phase is also identified in T-6 sample, although no indication of any crystalline Ta_2O_5 phase was observed in DTA traces. In this study, the average crystal size of crystallites was estimated from the analytical diffraction peak profiles by use of Scherrer equation, and the volume-weighted average crystallite sizes L_{hkl} , measured perpendicularly to the (hkl) lattice planes, were determined in correspondence with the (112) and (101) peak chosen for β -quartz s.s and Ta_2O_5 crystal phase, respectively. In addition, as the insert graph shown in Fig. 5, the reversed convolution transforms of the measured peak profiles were

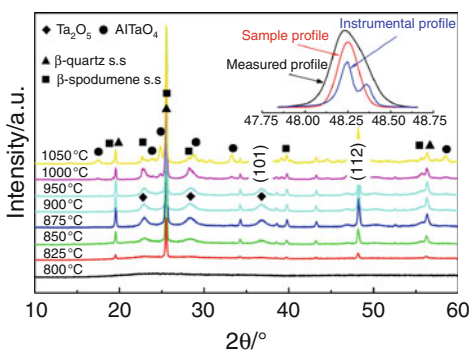


Fig. 5 XRD patterns of T-4 glasses crystallized at heating rate of 5 °C/min. Note the broad peaks corresponding to Ta_2O_5 . Insert graph shows the reversed convolution transform of (112) diffraction peak of β -quartz s.s phase

corrected for instrumental broadening. The peak broadening was attributed to crystallite size effects only.

Figure 6 shows the plots of volume-weighted average size for the β -quartz s.s and Ta_2O_5 crystals versus temperature for T-4 specimens. The average size of β -quartz s.s crystal is about 50–70 nm and increases slightly with heating temperature, while the crystallite growth with holding time is much more evident. The decrease at 1,050 °C is probably due to the fact that: β -quartz s.s transforms itself continuously into the correlated structure of β -spodumene s.s (consecutive transformation). On the contrary, the size of Ta_2O_5 crystallites is very small (7–15 nm), and increases slightly with the heating temperature. The notable increase of the sample crystallized at 1,000 or 1,050 °C is probably due to the formation and uncontrollable growth process of $AlTaO_4$ crystals at high temperature.

Unlike LAS glass with TiO_2 and ZrO_2 as nucleating agents [4], all the values of the average size of $ZrTiO_4$ at different temperatures are close to 4 nm, and each nucleus is isolated by the crystal growth of β -quartz s.s around. However, the size of Ta_2O_5 crystals increases with the heating temperature. As a result, the Ta_2O_5 crystalline phase identified by XRD is mainly attributed to the rejection and precipitation of Ta_2O_5 in residual glasses, and the Ta_2O_5 crystals distribute primarily within the spherulite (β -quartz s.s) boundary region. This result is in agreement with the study of Hsu and Speyer [18], that the rejection of redundant Ta_2O_5 into the amorphous matrix by growth of the large β -quartz s.s crystals and the other DTA exothermic peak corresponding to precipitation of Ta_2O_5 from the Tantalum-rich glass. Accordingly, the Ta_2O_5 rejection process by growth of β -quartz s.s regions and the precipitation of Ta_2O_5 crystalline phase are also suspected in T-4 sample as well, where exothermic peaks are overlapped.

It is well known that the effect of oxides on the crystallization mainly depends on the radius and electric charge

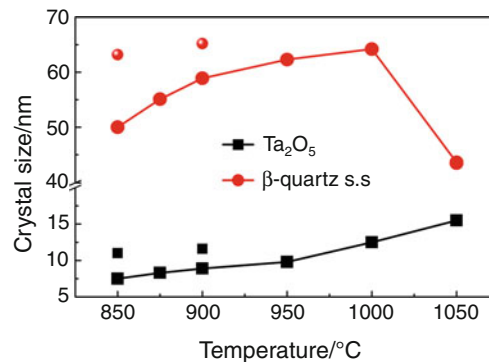


Fig. 6 Plots of the crystal size versus crystallization temperature for T-4 specimens under nonisothermal heat treatments. Note that the isolated values above curves correspond to the samples heated for a holding time of 1 h

of metal positive ions, and the metal positive ions with small radius and high field energy are easier to be encircled by regular oxygen ions. The radius (r) and field energy (z/r^2) of Ta^{5+} are 0.64 Å and 12.2, while that of Ti^{4+} are 0.605 Å and 10.7, and that of Zr^{4+} are 0.84 Å and 5.67, respectively. It would be quite natural to conclude that Ta^{5+} ions are easier to aggregate with oxygen ions to accelerate phase separation and form complete crystal phase as nuclei sites, as same as the mechanism of Ti^{4+} and Zr^{4+} ions. Naturally, tantalum oxide may be a good nucleation catalyst due to the aforementioned variation of coordination number with temperature, the charge difference between Ta^{5+} and Si^{4+} may also promote nucleation efficiency because of an unstable network structure causing phase separation. However, nucleation also occurs at much lower temperature and provides sufficient nuclei for subsequent crystallization, rather than only nucleation phase. Consequently, for Ta_2O_5 nucleating agents, the precipitation of a crystalline precursor phase acts as a site for nucleation and growth of β -quartz s.s., and the nucleation performance, as well as the effect of Ta_2O_5 on promoting crystallization are undoubtedly at low concentration of 4 mol%.

Microstructure

Microstructure not only plays a key role in determining the ultimate properties of glass-ceramics but also is useful to illustrate the behaviors of controlled nucleation and crystallization, including the distribution and morphology of crystals. The SEM micrographs for the three type samples are shown in Figs. 7, 8, and 9, respectively. The distinctions of morphology also show a very pronounced different mechanism of the crystallization and grain growth visually. As shown in Fig. 7a and b, a relatively coarse morphology, with needle-like or feather-like β -quartz s.s. crystals is obtained in T-2 sample heated at 1,000 °C/1 h. Figure 7c confirms the needle-like crystals with lengths of 1–2 µm and ~100 nm in diameter with uniform orientation. The microstructure, with cluster of dendritic crystal and lamellar structure, indicates a typical two-dimensional crystallization mechanism, which is in agreement with the above analysis of Avrami exponent ($n = 1.76$) for T-2 specimens. Therefore, when 2 mol% Ta_2O_5 is added for enhanced nucleation, the internal nucleation process as a precursor to crystallization is still relatively inefficient, the nucleation of β -quartz s.s. is initiated at surface sites, and uncontrolled crystallization of β -quartz s.s. and β -spodumen s.s. begins to grow from the surface of the glass toward the interior of the glass matrix above 950 °C.

Representative SEM micrographs of T-4 samples are presented in Fig. 8a–c, which are visually different from that of T-2 glass-ceramics. Owing to many nuclei with a

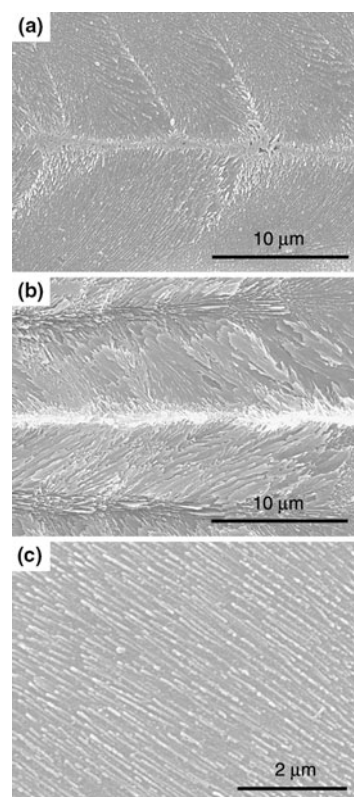


Fig. 7 SEM images of etched surfaces of T-2 glass-ceramics heat-treated at 1,000 °C. **a** dendritic crystals, **b** lamellar structure, and **c** needle-like crystals

nanometer size formed in prenucleation process, the next nucleation and growth of the metastable crystalline phases (β -quartz s.s.) result in a fine-grained crystal assemblage. After heated at 850 °C for 1 h, as shown in Fig. 8a, tiny sphere-shaped crystals precipitate with average size of 50–70 nm. In addition, crystallinity of this specimen is low, and the grain boundary is not distinct due to the large region of residual glass. With increasing temperature, the crystal size and crystallinity increase slightly (Fig. 8b), and the minor rod-like $AlTaO_4$ crystals (white region in Fig. 8c) form after heat-treated at 1,000 °C, coexisting with β -quartz s.s. and β -spodumen s.s. Compared with T-2 glass-ceramics, it is natural to conclude that Ta_2O_5 has a significant effect on the crystal size, crystal shape, and crystallinity of the LAS glass-ceramics. Moreover, with increase of Ta_2O_5 addition, the crystallization mechanism changes from surface crystallization to bulk crystallization, and these results confirm the above-mentioned results of crystallization kinetic analysis. As shown in Fig. 8a–c, it is remarkable that the micrographs of the bulk crystallized glass-ceramics are separated by the white spine-like region, resulting in the formation of network morphology in the homogeneous glass-ceramics. These spines are considered as the junction of two regions with different crystal orientation, and these zones, stacked by the totally crystallized

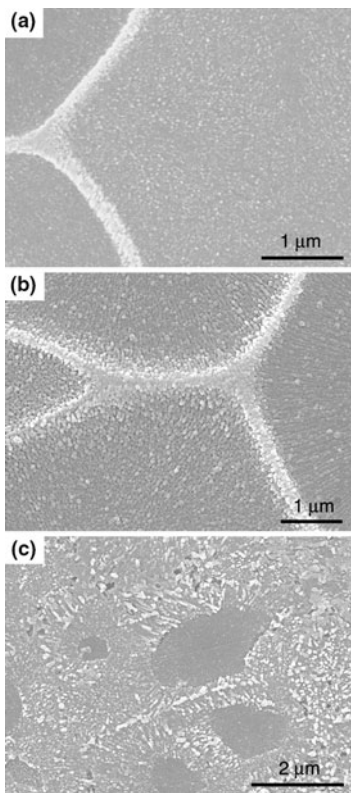


Fig. 8 SEM images of etched surfaces of T-4 glass-ceramics heat-treated at different temperatures for 1 h. **a** 850, **b** 900, and **c** 1,000 °C

grains, are less etched than the partially crystalline sphere around with residual glass, and appear slightly brighter in the electron beam. Furthermore, as shown in Fig. 8c, the secondary grain growth with temperature exhibits orientated movement, and the grain morphology appear an ordered arrangement and impingement around the spines.

The microstructure evolutions of T-6 glass-ceramics are similar to that of T-4 samples, and moreover, by comparing the two graphs (Figs. 8a and 9a), the crystallinity of T-6 samples is higher than that of T-4 under the same heating procedure. In addition, the uniformly distributed crystals with 50–70 nm in diameter are shown in Fig. 9a and b, and the grain boundaries appear slightly darker in electron beam owing to the corrosion of the residual glass phase after HF-etching. Unfortunately, the tiny crystals of Ta_2O_5 phase, dispersing uniformly throughout a continuous residual glass matrix, are not visually observed in SEM micrographs. In fact, the diffusion of tantalum is expected to be slow in such a viscous glass, and the formation of Ta_2O_5 crystallites is a rate-limiting process of grain growth of β -quartz s.s. As a result, the small size of Ta_2O_5 crystals is naturally accepted. In addition, during the growth of β -quartz s.s, the substitution of Si by Al in the crystalline phase is limited by the supply of Li, and the “glass-like” intergranular regions enriched in aluminum have also been found [28]. Thus, as shown in

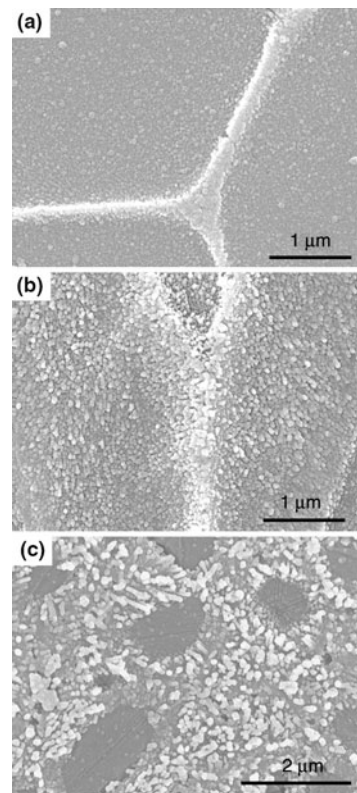


Fig. 9 SEM images of etched surfaces of T-6 glass-ceramics heat-treated at different temperatures for 1 h. **a** 850, **b** 900, and **c** 1,000 °C

Fig. 9c, the precipitation of $AlTaO_4$ (white crystals) in the aluminum and tantalum-rich residual glasses is reasonable. Meanwhile, the region of residual glass is limited in small scale, which could be interpreted as a mechanism of inhibiting grain growth of $AlTaO_4$. However, there are few reports about the secondary grain growth of the LAS glass-ceramics [29]. Therefore, the details of mechanism of the secondary grain growth and the formation of this novel morphology patterns in tantalum-containing glass-ceramics will be studied further.

Conclusions

The glass-ceramics based on the $Li_2O-Al_2O_3-SiO_2$ system were prepared by using Ta_2O_5 as nucleating agent. The obtained results of crystallization mechanism and microstructure evolution are summarized as follows:

1. Ta_2O_5 has a good efficiency in promoting crystallization of LAS glasses, and gives the sequence of crystallization with increasing temperature as follows: phase separation followed by the formation of precursor nuclei, the crystallization of β -quartz s.s along with additional precipitation of Ta_2O_5 within grain boundary, and

- eventually the phase transformation from β -quartz s.s to β -spodumene s.s, and the formation of AlTaO_4 crystals.
2. With the increasing amount of Ta_2O_5 from 2 to 6 mol%, the crystallization activation energy decreased from 297.73 to 218.66 kJ mol $^{-1}$, while the crystallization index increased from 1.76 to 3.39, which indicated that the crystallization mechanism changed from surface crystallization to internal crystallization.
 3. The amount of Ta_2O_5 has a pronounced effect on the microstructure: the cluster of dendritic crystal and lamellar structure obtained in T-2 glass-ceramics indicate a typical two-dimensional crystallization mechanism, whereas fine-grained microstructure obtained for T-4 specimens is due to bulk crystallization mechanism.
 4. In addition, the effects of Ta_2O_5 on nucleation and crystallization are mainly attributed to the precipitation of crystalline precursor phase (Ta_2O_5), as nuclei of the subsequent crystal growth. The precipitation of tiny Ta_2O_5 crystals is mainly attributed to the concentration of tantalum in residual glass, rejected from the growing β -quartz solid solution.

References

1. McMillan PW. Glass-ceramics. 2nd ed. London: Academic Press; 1979.
2. Stookey SD. Catalyzed crystallization of glass in theory and practice. *Ind Eng Chem*. 1959;51:805–8.
3. Beall George H., Pinckney Linda R. Nanophase glass-ceramics. *J Am Ceram Soc*. 1999;82:5–16.
4. Riello P, Canton P, Comelato N, Polizzi S, Verita M, Fagherazzi G, et al. Nucleation and crystallization behavior of glass-ceramic materials in the $\text{Li}_2\text{O}-\text{Al}_2\text{O}_3-\text{SiO}_2$ system of interest for their transparency properties. *J Non-Cryst Solids*. 2001;288:127–39.
5. Pinckney Linda R., Beall George H. Microstructural evolution in some silicate glass-ceramics: a review. *J Am Ceram Soc*. 2008;91:773–9.
6. Nordmann Astrid, Cheng Yi-Bing. Crystallization behaviour and microstructural evolution of a $\text{Li}_2\text{O}-\text{Al}_2\text{O}_3-\text{SiO}_2$ glass derived from spodumene mineral. *J Mater Sci*. 1997;32:83–9.
7. Guedes M, Ferro AC, Ferreira JMF. Nucleation and crystal growth in commercial LAS compositions. *J Eur Ceram Soc*. 2001;21:1187–94.
8. Hu AM, Li M, Mao DL. Crystallization of spodumene-diopside in the LAS glass ceramics with CaO and MgO addition. *J Therm Anal Calorim*. 2007;90:185–9.
9. Anmin H, Ming L, Dali M. Phase transformation in spodumene-diopside glass. *J Therm Anal Calorim*. 2006;84:497–501.
10. Guo Xingzhong, Yang Hui, Han Chen, Song Fangfang. Nucleation of lithium aluminosilicate glass containing complex nucleation agent. *Ceram Int*. 2007;33:1375–9.
11. Apel Elke, Hoen Christian Vant, Rheinberger Volker, Holand Wolfram. Influence of ZrO_2 on the crystallization and properties of lithium disilicate glass-ceramics derived from a multi-component system. *J Eur Ceram Soc*. 2007;27:1571–7.
12. Doherty PE, Lee DW, Davis RS. Direct observation of the crystallization of $\text{Li}_2\text{O}-\text{Al}_2\text{O}_3-\text{SiO}_2$ glasses containing TiO_2 . *J Am Ceram Soc*. 1967;50:77–81.
13. Hu AM, Liang KM, Wang G, Zhou F, Peng F. Effect of nucleating agents on the crystallization of $\text{Li}_2\text{O}-\text{Al}_2\text{O}_3-\text{SiO}_2$ system glass. *J Therm Anal Calorim*. 2004;78:991–7.
14. Maier V, Muller G. Mechanism of oxide nucleation in lithium aluminosilicate glass-ceramics. *J Am Ceram Soc*. 1987;70:176–8.
15. Arnault L, Gerland M, Riviere A. Mechanism of oxide nucleation in lithium aluminosilicate glass-ceramics. *J Mater Sci*. 2000;35: 2331–45.
16. Zheng X, Wen G, Song L, Huang XX. Effects of P_2O_5 and heat treatment on crystallization and microstructure in lithium disilicate glass ceramics. *Acta Mater*. 2008;56:549–58.
17. An-Min Hu, Kai-Ming Liang, Fei Peng, Guo-Liang Wang, Hua Shao. Crystallization and microstructure changes in fluorine-containing $\text{Li}_2\text{O}-\text{Al}_2\text{O}_3-\text{SiO}_2$ glasses. *Thermochim Acta*. 2004;413:53–5.
18. Hsu Jen-Yan, Speyer Robert F. Comparison of the effects of titania and tantalum oxide nucleating agents on the crystallization of $\text{Li}_2\text{O}-\text{Al}_2\text{O}_3-6\text{SiO}_2$ glasses. *J Am Ceram Soc*. 1989;72:2334–41.
19. Donald IW, Metcalfe BL, Gerrard LA, Fong SK. The influence of Ta_2O_5 additions on the thermal properties and crystallization kinetics of a lithium zinc silicate glass. *J Non-Cryst Solids*. 2008;354:301–10.
20. Zivanovic VD, Grujic SR, Tasic MB, Blagojevic NS, Nikolic JD. Non-isothermal crystallization of $\text{K}_2\text{O}\cdot\text{TiO}_2\cdot3\text{GeO}_2$ glass. *J Therm Anal Calorim*. 2009;96:427–32.
21. Nitsch K, Rodova M. Crystallization study of Na-Gd phosphate glass using non-isothermal DTA. *J Therm Anal Calorim*. 2008;91:137–40.
22. Davis Mark J. Crystallization measurements using DTA methods: applications to Zerodur. *J Am Ceram Soc*. 2003;86:1540–6.
23. Araujo EB, Idalgo E. Non-isothermal studies on crystallization kinetics of tellurite $^{20}\text{Li}_2\text{O}-^{80}\text{TeO}_2$ glass. *J Therm Anal Calorim*. 2009;95:37–42.
24. Soliman AA. Derivation of the Kissinger equation for non-isothermal glass transition peaks. *J Therm Anal Calorim*. 2007;89:389–92.
25. Pacurariu C, Lazau RI, Lazau I, Tita D. Kinetics of non-isothermal crystallization of some glass-ceramics based on basalt. *J Therm Anal Calorim*. 2007;88:647–52.
26. Kissinger HE. Variation of peak temperature with heating rate in differential thermal analysis. *J Res Natl Bureau Stand*. 1956;57: 217–21.
27. Augis JA, Bennett JE. Calculation of the Avrami parameters for heterogeneous solid-state reactions using a modification of the Kissinger method. *J Therm Anal Calorim*. 1978;13:283–92.
28. Chen QQ, Gai PL, Groves GW. Microstructure and grain growth in $\text{Li}_2\text{O}-\text{Al}_2\text{O}_3-\text{SiO}_2$ glass ceramics. *J Mater Sci*. 1982;17:2671–6.
29. Chuyung CK. Secondary grain growth of $\text{Li}_2\text{O}-\text{Al}_2\text{O}_3-\text{SiO}-\text{TiO}_2$ glass-ceramics. *J Am Ceram Soc*. 1969;52:242–5.